Nonlinear optical properties of electrochemically synthesized Au nanoparticles

J. W. DADGE[a], M. ISLAM[b], A. K. DHARMADHIKARI[c], S. R. MAHAMUNI[b], R. C. AIYER[b,*]

[a]Department of Physics, College of Engineering, Shivaji Nagar, Pune 411 005, India
[b] Department of Physics, University of Pune, Pune 411 007, India
[c] Atomic and Molecular Sciences Group, Tata Institute of Fundamental Research,
Mumbai 400 005, India

The second harmonic generation (SHG) in electrochemically synthesized gold nanoparticles capped in Tetraoctylammoniumbromide (TOAB), in colloidal form using nanosecond Nd: YAG laser, is reported. The effect of particles size (6, 10 and 20 nm) in different solvents on SHG is investigated. The SHG as a function of concentration, angular distribution and its polarization properties for 6 nm size in Dimethylformamide(DMF) is studied. Dependence of SHG on $(R)^6$ is simulated, matches with the experimental results. By Hyper Rayleigh Scattering (HRS) the β (first order optical hyperpolarizability) value is found to be 2.68×10^{-19} esu for 6nm, which is an order of magnitude higher than that reported for gold particles.

1. Introduction

The size and shape dependent optical and electronic properties of metal nanoparticles have attracted a lot of research attention [1-4]. Au, Ag and Cu clusters show characteristic surface plasmon absorption in the visible–near infrared wavelength region, known to cause a highly localized electrical field at the interface between the metal surface and surrounding medium [5]. The metal clusters have close lying bands allowing electrons to move freely. The oscillations of free electrons in the conduction band occupying energy states near the Fermi level give rise to surface plasmon absorption band (sp), which depends on size and the chemical surroundings of the metal nanoparticles [6,7]. Enhanced optical nonlinearity arises from the enhancement of local field near the surface plasmon resonance. The optical nonlinear properties have been extensively studied in Au nanoparticles [8-11]. The silver metal liquid like films show intense SHG signal than smooth and roughened surface silver films [12]. Further, the dependence of the SHG on the shape of nanoparticles is investigated recently [13] stating that SHG from ellipsoidal Ag nanoparticles embedded in silica glass show nearly three orders of magnitude enhancement than that in the smooth Ag surfaces. Antoine *et al.* [9] have observed SHG at the air/toluene interface and embedded in an aluminum matrix in reflected mode and Anceau *et al.* [10] have observed SHG enhancement in the gold nanostructures probed by two-photon microscopy.

Hyper Rayleigh Scattering is a nonlinear incoherent second order light scattering that is used to study the second order nonlinear optical properties of molecules or nanoparticles in solution [14]. The generation of HRS relies upon the fluctuations of the density or orientation of molecules or nanoparticles, which instantaneously break the centrosymmetry of isotropic media and create conditions of net frequency doubling. A problem with the experimental determination of the first order optical hyperpolarizability β (second order nonlinear optical polarizability) lies in the fact that centrosymmetric structures of individual molecules with a nonzero microscopic hyperpolarizability β do not possess a macroscopic second order nonlinear optical (NLO) susceptibility B. Therefore, the first measurements of B were performed on crystals without centrosymmetry, Langmuir-Blodgett films, and poled polymers [14,15]. However the Kurtz powder method generated substantial amount of second harmonic powder efficiency data [16]. Compared to the conventional technique of electric field induced second harmonic generation, the HRS method offers advantages, in particular, it can be performed in a liquid phase without the need of application of an aligning electric field. The electric field induced second harmonic generation (EFISHG) is the only technique to determine hyperpolarizabilities in solution [14]. Consequently, HRS has been successfully used to determine β value of gold nanoparticles. Semiconductor or metal nanoparticles exhibit interesting optical properties due to the confinement of the electronic wave functions, the drastically changed surface to volume ratio, and their surface conditions [17].

In this paper, to the best of our knowledge the first example of gold nanoparticles in colloids by employing the simple electrochemical method along with their β is reported. Which is found to be an order of magnitude higher than those reported for gold particles in the

colloidal form.   The UV-Vis absorption peak, and SHG from Au nanoparticles capped in TOAB in the colloidal form as a function of size, surrounding media and concentration (6 nm) is reported. Dependence of SHG on (R^6) is simulated, the experimental results match with it.

2. Experimental

Gold nanoparticles of different sizes were synthesized using the electrochemical method described by M. T. Reetz et al. [18]. The electrochemical route is briefly explained as follows. Au electrode was used as a sacrificial anode, in an electrochemical bath comprising of acetonitrile and Tetrahydrofuran (THF), in the ratio 4:1, while Platinum (Pt) was used as a cathode. The capping agent, TOAB also served as an electrolyte. Electrolysis was carried out under Nitrogen atmosphere for a few hours, in constant current mode (10mA to 40mA/cm^2), with constant stirring (for uniform dispersion of particles), quantitative dissolution of the gold anode occurs resulting in black precipitate. The dispersion was washed at least three times with acetronitrile to remove the reaction by products.

Size estimation and structural studies of the nanoparticles were carried out by x-ray diffraction (XRD) as well as transmission electron microscopy (TEM), scanning electron microscopy (SEM) with energy dispersive x-ray spectroscopy (EDS) studies to check purity of the particles. The shape of the particles is spherical.
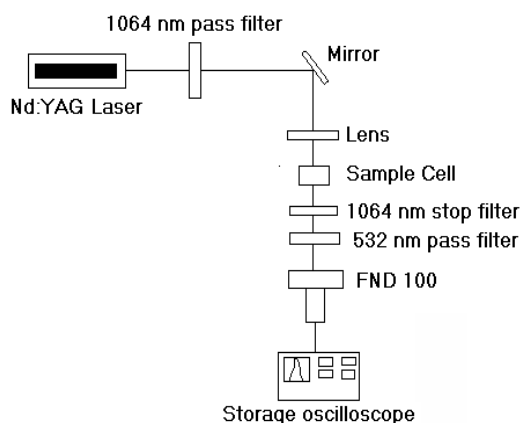

Fig .1 Experimental setup for HRS and SHG.

The experimental setup is shown schematically in Fig.1 for coherent SHG and HRS, consists of a Q-switched Nd:YAG laser (λ = 1064nm) 1 to 100mJ pulse energy, 1Hz repetition rate, and 20ns pulse width [19-22]. The laser radiation was filtered by a 1064nm pass filter (Melles Griot) to minimize the background intensity. The laser beam was focused using a lens (focal length 14cm) on a 10 x10 x1 mm^3 borosilicate cuvette containing nanoparticles in the colloidal form for coherent SHG. The signal

generated in the visible range was detected through a monocromator with photomultiplier tube through a 530 nm pass filter and measured on a fast storage oscilloscope (THS 730A). The coherence was confirmed by using a polarizer. The coherent SHG measurements of gold nanopaticles were carried out for 6nm and 10nm size particles in different organic solvents.

The HRS measurements of 6nm size nanoparticles were carried out in Methanol by the methods described [23-26]. The laser beam was focused on a 10 x10 x 45mm^3 quartz cuvette using lens (Focal length 14cm) containing nanocrystallites in the colloidal form. The HRS signal generated was focused onto a detector (FND 100) which was at the right angle to the fundamental beam through a 532 nm pass filter (Melles Griot) and measured using Tecktronix fast storage oscilloscope (THS 730A).

3. Results and discussion

XRD peak positions are consistent with those of bulk gold [27]. No other phase or element was identified, confirming that TOAB prevents agglomeration and oxidation of gold nanoparticles [28]. The lattice contraction of about 2% was observed due to the size reduction. The average particles sizes were estimated by Scherrer formula [29] and confirmed by TEM to be of 6 ± 1, 10 ± 1.5 and 20 ± 2 nm.

Optical absorption spectra of 6, 10 and 20 nm in acetonitrile show (Fig. 2) peak maxima at 530, 525 and 520nm respectively. The shift in the plasmon band to lower wavelength for 6 nm agrees with the Mie's theory modified by Kreibig et al. [30] ,due to the change in dielectric constant with the size of the metal particles, which is a function of interband (d electrons) and intraband (free electrons) electrons. The number of free electrons is a function of size of the clusters [31].
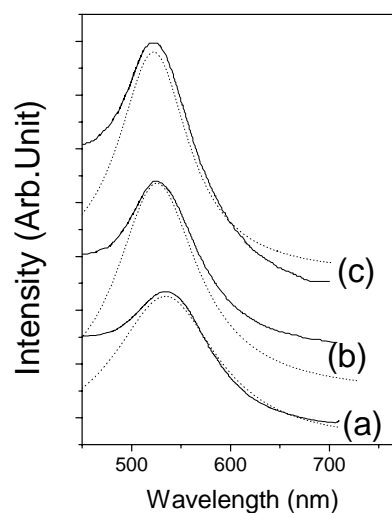

Fig. 2. Solid lines represents experimental optical absorption spectra of Au nanoparticles and dot lines represents simulated spectra of having average size of (a) 6 and (b) 10 nm and (c) 20 nm.

The spectra were simulated for the value of bulk plasma frequency, $\omega_p = 1.36 \times 10^{16}$ s^{-1}, electron velocity at Fermi level $v_F = 1.39 \times 10^6$ m s^{-1} and electronic mean free path as the size of particles, show peaks at 530, 525 and 520 for 6,10 and 20nm respectively.

Au nanoparticles suspended in solvents having wide range of refractive index show the surface plasmon band between 500 and 550 nm [32]. In the present study it was observed to vary as DMF (522 nm), toluene (530 nm), acetonitrile (530 nm), ethanol (521 nm) and DMSO (521 nm) for 6 nm size. These solvents do not interact with the surface of the gold nanoparticles and shift the absorption peak towards longer wavelengths with increasing refractive index of the solvent [28]. The location of the plasmon absorption band is discussed within the framework of Drude model [33].

$$\lambda^2 = \lambda_p^{\,2}(\varepsilon^\infty + 2\varepsilon_m) \qquad (1)$$

where λ_p is the metal's bulk plasma wavelength, ε^∞ the high frequency dielectric constant due to interband and core transitions, and ε_m is the medium dielectric constant. ($n = (\varepsilon_m)^{1/2}$, n its refractive index). Solvents forming complex with Au nanoparticles alter the refractive index of the surroundings.

Murray and co-workers [34] modified the Drude equation to account the contribution of capping agent:

$$\lambda^2 = \lambda_p^{\,2}[(\varepsilon^\infty + 2\varepsilon_m) - 2g(\varepsilon_m - \varepsilon_s)/3] \qquad (2)$$

where g is the volume fraction of the shell layer. In the present case, TOAB-capped gold nanoparticles might have got stabilized through noncovalent interaction to render the solvent molecules to penetrate through the shell and influence the surface plasmon (SP) band.

Fig. 3 shows SHG variation in 6 and 10 nm size (inset) gold nanoparticles as function of incident energy in different solvents. In the present case, enhancement of SHG signal due to resonance with surface plasmon band located at the 530 nm wavelength is observed in the forward direction. The SHG intensity varies as square of the input intensity, the pulse width of fundamental beam and 2ω beam was found to be the same confirming the second harmonic generation (measured on FND-100 with appropriate filters). The enhancement of SHG could be explained as follows:

At the plasmon resonance frequency, non-linear polarization contribution dominates over the volume contribution, with a net enhancement compared to the non-resonant case. The output of second harmonic power for spherical particles is given by [35]

$$S = \frac{3ce^2 \left| E^{(i)} \right|^4}{m_e^{\,2}} \left(\frac{2R}{c} \right)^6 \omega^2 (A + B) \qquad (3)$$

where

$$A = \left| \frac{1 - \varepsilon(2\omega)}{[\varepsilon(\omega) + 2][\varepsilon(2\omega) + 2]} \right|^2$$

$$B = \frac{36}{5} \left| \frac{\varepsilon(\omega) - 1}{[\varepsilon(\omega) + 2]^2 [2\varepsilon(2\omega) + 3]} \right|^2$$

where $E^{(i)}$ is the intensity of the electric field at the surface, ε is the complex dielectric function of the particles, ω is the frequency of the exciting radiation, 2ω is the second harmonic frequency, m_e is the effective mass of the electron, R is radius of particles, c is the velocity of light and e is the electronic charge. For particles in a medium of relative permittivity ε_m the dielectric function in equation is the permittivity relative to that of the medium $\varepsilon_{rel} = \varepsilon/\varepsilon_m$.
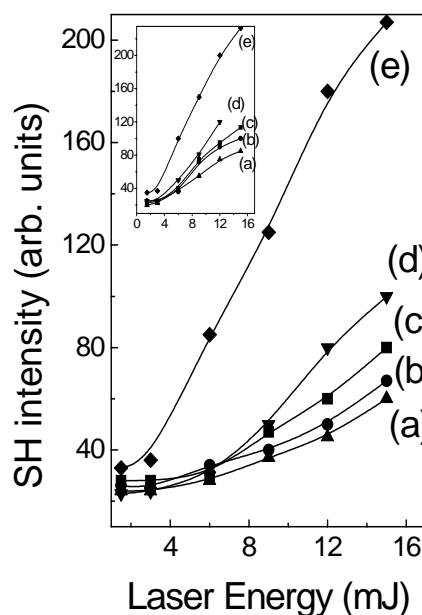

Fig. 3 SHG of 6 and 10 nm (inset) gold nanoparticles in different solvents (a) DMSO (b) DMF (c) Acetonitrile (d) Ethanol (e) Toluene. (Inset 10 nm gold nanoparticles SHG)

In the present study a plot of log of SHG intensity per cluster versus log of 2R exhibits a straight line giving the slope of 3 (inset Fig.4). By calculating the term A and B in eq.3 for 6, 10 and 20 nm sized particles gives the ratios of 1.6×10^{-4} : 0.42676, 1.5×10^{-4} : 0.4449, and 1.4×10^{-4} : 0.4485 respectively revealing the surface domination over the volume contribution.
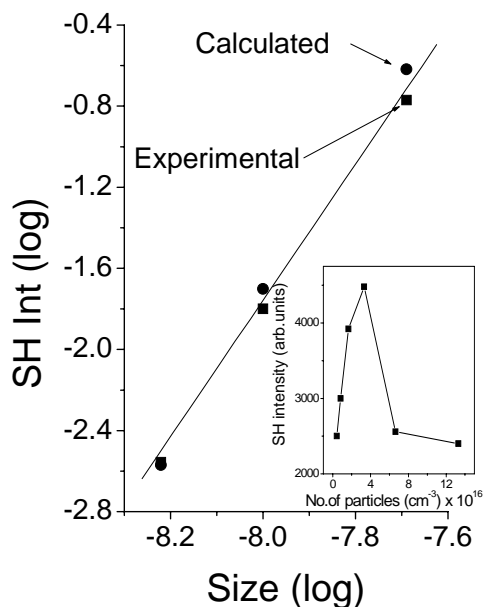
Fig.4 SH intensity per cluster vs radius of gold nanoparticles in DMF. (inset) Concentration dependent SHG in gold nanoparticles having size of 6 nm in DMF.

We have also simulated SH intensity by using equ.3 and the dielectric function of gold clusters as a function of wavelength given by $\varepsilon(\omega) = \varepsilon'_1(\omega) + i\varepsilon'_2(\omega)$
where

$$\varepsilon_1(\omega) = \varepsilon_1'(\omega) + 1 - \frac{\omega_p^2}{\omega^2 + \omega_c^2} \quad (4)$$

$$\varepsilon_2(\omega) = \varepsilon_2'(\omega) + \frac{\omega_p^2 \omega_c}{\omega(\omega^2 + \omega_c^2)} \quad \text{with} \quad \omega_c = \frac{v_f}{L} + \frac{2v_f}{d}$$

Where $\varepsilon'_1(\omega)$ and $\varepsilon'_2(\omega)$ [$\varepsilon_1(\omega)$ and $\varepsilon_2(\omega)$] are the real and imaginary parts of the dielectric constant of the nanoparticles [bulk] gold, ω_p is the bulk plasma frequency ($\omega_p = 1.36 \times 10^{16} s^{-1}$ for gold), c is the velocity of light in vacuum, and v_f the Fermi velocity (1.4×10^6 ms^{-1} for gold). L is the electron mean free path . Following report by Kreibig size dependence was taken into account by using the relation L= 2d/3. The above relation, predicts the existence of the resonance SP peak, In this calculation. The peak positions were produced at 532, 542 and 548 nm having amplitude of 100, 94 and 82% at 532 nm.[Fig.5]. Therefore, with 1064 nm incident wavelength coherent SHG was obtained at 532 nm. The bandwidth was found much narrow than absorption spectrum which is good agreement with the Antoine et al.[9]

Besides surface plasmon contribution electron-phonon interactions might be contributing to the phenomena [36]. The surface passivation [28] is an additional possible source for the enhancement of the SHG response in

nanoparticles. In particular, dangling orbitals of passivated sites on the nanoparticles surface are highly polarizable which may contribute substantially to the second order nonlinear signals.

SH signal as a function of size in DMF shows increase in SH intensity with the size of the nanoparticles [inset Fig. 4] due to the number of atoms residing on the surface and contributing towards SH generation. e.g.10 nm radius: 244672 atoms with 15017 surface atoms, 3 nm radius: 6607 atoms with 1351 as surface.

Present results show highest intensity of SHG in toluene. (Fig. 3) Toluene has highest refractive index. The field experienced inside the nanoparticles will therefore be highest giving rise to highest SHG intensity. This is followed by Ethanol and Acetonitrile. Diemethyl sulfoxide (DMSO) and DMF, in spite of their higher refractive indices offer low SHG, DMSO giving the least (Table.1). This can occur only if there is direct interaction of the polar solvents with the gold surface. Such complexation processes may override the effects of refractive index since it substantially alters the electron density of the gold nanoparticles surface. Also these are lossy dielectric materials.

Table 1 SHG intensity in various solvents for TOAB capped Au nanoparticles for 15 mJ energy

Solvent	Index of refraction (n)	SHG intensity at 15mJ for 6 nm size (arb. units)
Toluene	1.49	207
Ethanol	1.35	100
Acetonitrile	1.34	80
DMF	1.43	67
DMSO	1.47	60

Figure 4B (inset) shows the SHG intensity as a function of concentration of gold nanoparticles (6 nm in DMF). At concentrations ranging from 0.39×10^{16} particles/cm^3 to 3.25×10^{16} particles/cm^3, the intensity increases. At further higher concentrations, the intensity tends to decrease because of the absorbance at the fundamental and harmonic wavelength [37].

In a solution containing nanoparticles, no phase relationship exists between the particles, hence no coherent signal can be collected, the incoherent harmonic signal, known as the Hyper Rayleigh signal, scattered by the solution in a right angle direction to the fundamental

incident beam has been detected from a monodispersed solution of nanoparticles.

A quadratic dependence of the HRS signal $I^{2\omega}$ on the incident light intensity I^{ω} is always observed, according to $I^{2\omega} = GB^2 (I^{\omega})^2$, with G a proportionality constant, containing geometrical and electronic factors. For a two component system,

$$B^2 = N_{solvent} \beta^2_{solvent} + N_{solute} \beta^2_{solute} \qquad (4)$$

For the low concentration used, the presence of the solute molecules do not significantly change the number density $N_{solvent}$ of the solvent molecules. Measurements at different number densities of the solute then show a linear dependence of GB^2 on N_{solute}. From the intercept and the slope, β_{solute} is calculated [38-40], when $\beta_{solvent}$ is known, or vice versa. Since no external field directing the dipoles has to be applied, the local field correction factor at zero frequency is eliminated. The only local field correction factors needed are those at optical frequencies, which can be estimated by the standard methods [15]. The internal reference method (IRM) eliminates the need for local field correction factors, since these factors are divided out by calibrating and measuring in nearly the same local field, as long as the number density of the solute molecules present does not significantly change the refractive index of the solution.
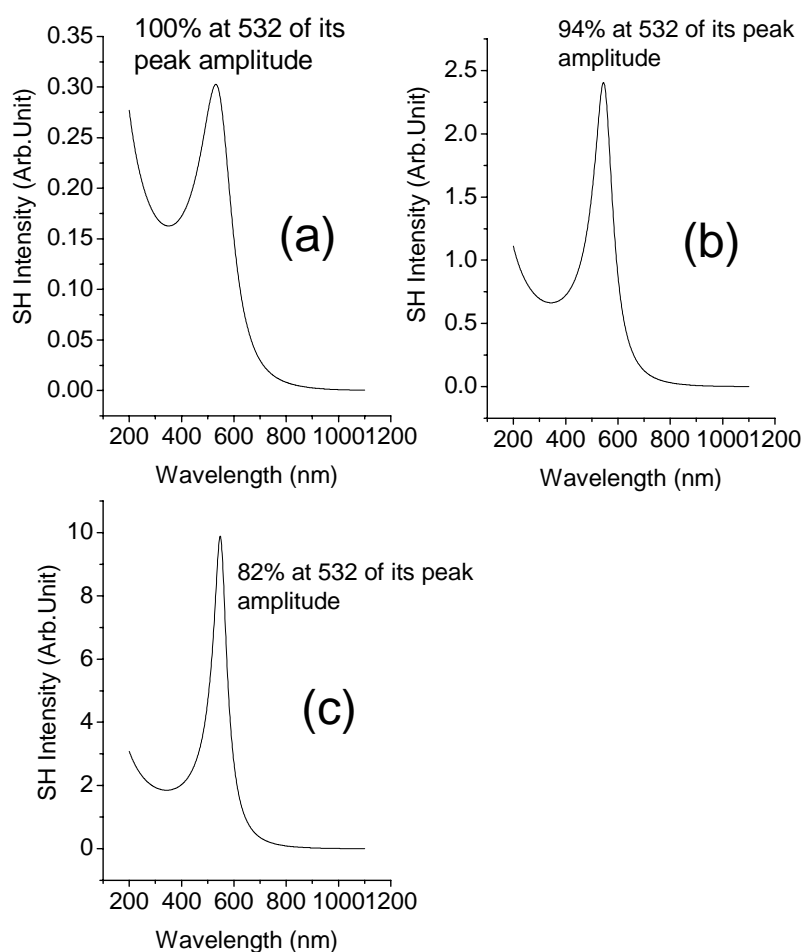

Fig.5 Simulated SHG of (a) 6 nm (b) 10 and (c) 20 nm size Au particles in Tolune.

To ascertain that the results of our measurements are consistent with the accepted data, we have calibrated our experiment by using paranitroaniline (p-NA) dissolved in methanol as the sample. The obtained value of β of p-NA to be 9.1×10^{-30} esu, which was in satisfactory agreement with the literature value [41]. The quadratic dependence of the observed HRS signal $I^{2\omega}$ at optical frequency 2ω on incident intensity I^{ω} at frequency ω is illustrated in Fig. 6 for gold partarticles in methanol. The measurements were repeated at least thrice and were found to be reproducible with the accuracy of ± 4% (second harmonic intensity). The expected linear dependence of the retrieved value for

the quadratic coefficient GB^2 on the number density N_{solute} is shown in Fig. 7. The hyperpolarizability of a single nanoparticle was then obtained provided the hyperpolarizability of a methanol molecule is known. With the value of $\beta_{solvent} = 0.69 \times 10^{-30}$esu, we were able to deduce the method of extracting accurate values for β_{solute} by the IRM. The value for gold particle β_{gold} 2.68 X 10^{-19} esu with a diameter of 6nm, which is   higher than the reported ones [24].
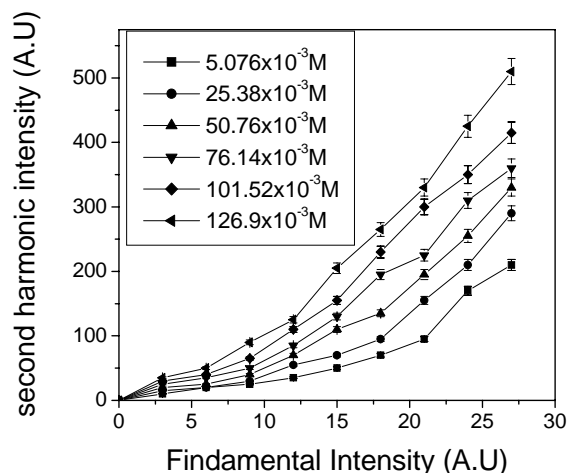

Fig. 6 Incoherent SHG in solution for Au Nanocrystallites in methanol.
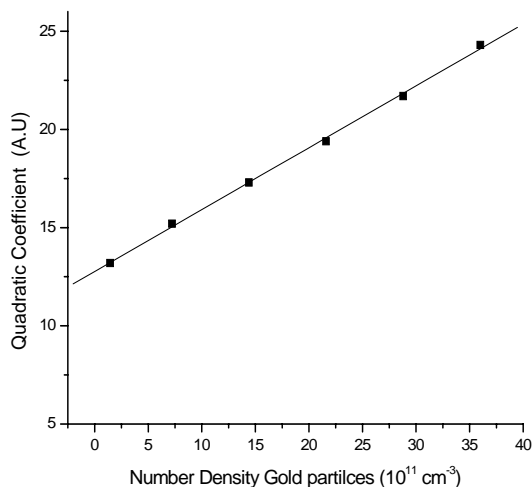

Fig. 7. Quadratic Coefficient GB^2 obtained from the curves in fig.6, vs number density of gold particles in methanol.

It is known that the HRS method relies upon random density fluctuations to create condition compatible with net frequency doubled. For each scatterer in solution, a substantial requirement for the finite HRS is the presence of noncentrosymmtric structure. The gold nanoparticles studied here have the cubic structutre. However, the continuity of crystalline lattice is broken at the surface for nanoparticles, resulting in their second order NLO response drastically differing from those of the corresponding nanocrystalline substance.

As reported, surface termination of the crystalline lattice creates a condition of noncentrosymmetry which contributes to the large β values [42,43]. The literture [44] also indicated that the electron distribution around surface atoms is inherently highly noncentrosymmetric. Moreover an important feature of nanoscale particles is the enhanced ratio of the surface atoms to volume atoms. These show that nanoparticles surface atoms play an important role in the contribution to the HRS signal.

4. Conclusion

Gold nanoparticles using electrochemical method are successfully synthesized.

Au nanoparticles disperse in different solvents offer coherent SHG in the forward direction. Toluene offers the highest coherent SHG because of highest refractive index. DMSO and DMF being polar, though have higher refractive index, offer the lower SHG because they interact with gold surfaces and override the effect of refractive index and also these are lossy dielectric materials. Jha's theory [35] experimentally verified in colloidal solution for coherent SHG in the forward direction. Using the HRS technique, very large second order NLO response of gold nanoparticles was exhibited. The β_{gold} 2.68 X 10^{-19} esu, in methanol is calculated which seems to come from the method of synthesis. This offers considerable potential of gold nanoparticles in NLO applications.

References

[1] M.A. El Sayed, Acct. Chem. Res**. 34**, 257 (2001).
[2] C. N. R. Rao, G. U. Kulkarni, P.J. Thomson,
    P.T. Edwards, Chem. Eur. J **8**, 29 (2002).
[3] Y. Joseph, I. Besnard, M. Rosenberger, B. Guse,
    H-G. Nothofer, J. M. Wessels, U. Wild,A. Knop-
    Gericke, D. Su, R. Schlögl, A. Yasuda,
    T. Vossmeyer, J. Phys. Chem B **107**, 7406 (2003).
[4] S. R. Nicewarner-Peña, A. J. Carado, K. E. Shale,
    C. D. Keating, J. Phys. Chem. B **107**, 7360 (2003).
[5] K. Murakoshi, H. Tanaka, Y. Sawai, Y. Nakato, J.
    Phys. Chem. B **106**, 3041 (2002).
[6] K. L. Kelly, E. Coronado, L. Zhao, G. C. Schatz,
    J. Phys. Chem. B **107**, 668 (2003).
[7] A. Hilger, M. Tenfelde, U. Kreibig, Appl. Phys.
    B **73**, 361 (2001).

[8] S. Qu, C. Zhao, X. Jiang, G. Fang, Y. Gao, H. Zeng, Y. Song, J. Qiu, C. Zhu , K. Hirao, Chem. Phys. Lett. **368**, 352 (2003).

[9] (a)R. Antoine, P. F. Brevet, H. Girault, D. Bethell , D. J. Schiffrin, Chem. Comm. (1997) 1901. (b) R. Antonie, M. Pellarin, B. Plapant, M. Broyer, B. Prevel, P. Galleto,P. F. Brevet, H.H.Giraut, J. Appl. Phys. **84**, 4532 (1998).

[10] C. Anceau , S. Brasselet , J. Zyss, P. Gadenne, Opt. Lett. **28**, 713 (2003).

[11] P. Galletto, P. F. Brevet, H. H. Girault, R. Antoine, M. Broyer, Chem. Comm. 581 (1999).

[12] R. Bavli, D. Yogev, S. Efrima, G. Berkovic, J. Phys. Chem. **95**, 7422 (1995-II).

[13] J. Podlipensky, G. Lange, S. H. Graener, I. Cravetchi, Opt. Lett. **28**, 716 (2003).

[14] Koen Clays and Andre Persoons, Phys. Rev. Lett. **66**, 2980 (1991).

[15] D. J.Williams, Angew. Chem.Int.Ed. Engl. **23**, 690 (1984).

[16] J.R.Nicoud and R.J.Twieg, Nonlinear Optical Properties of Organic Molecules and Crystals, edited by D.S.Chemlaand Z.Zyss (Academic, Orlando, FL, 1987),Vol. 2. pp.221-224.

[17] Xin Wang, Yu Zhang, Degang Fu, Zuhong Lu, Yiping Cui, Proc. SPIE Photonics Technology. **3899**, 384 (1999).

[18] M. T. Reetz, W. Helbig, J. Am. Chem. Soc. **116**, 7401 (1996).

[19] Q. Song, C. wan, and C. K. Johnson, J. Phys. Chem. **98**, 1999 (1994).

[20] H.Wang et al. Chem. Phys. Lett. **15**, 259 (1996).

[21] S. Pethkar, J.A. Dharmadhikari, A.A. Athawale, R.C. Aiyer, and K. Vijayamohanan, J. Phys. Chem. B **105**, 5110 (2001).

[22] M.L. Sandrock, C. D. Pibel, F. M. Geiger, C. A. Fross (Jr), J. Phy. Chem. B **103**, 2668 (1999).

[23] W. Terhune, P. D. Maker, and C. M. Savage, Phys. Rev. Lett. **14**, 681 (1965).

[24] M. H. Rouillat, I.R. Antoine, E. Benichou, P.F. Brevet, Analy. Sci. **17,** i235 (2001).

[25] P. Galletto, P. F. Brevet, H. H. Girault, R. Antoine, M. Broyer, Chem. Comm.581, (1999).

[26] C.X.Zhang, Y. Zhang, X.Wang, Z. M. Tang, Z.H. Lu, Analy. Biochem. **320**, 136 (2003).

[27] Powder diffraction files (4 – 784 for gold) 1984. U.S.A.

[28] K.G. Thomas, J. Zajicek, P.V. Kamat, Langmuir **18**, 3722 (2002).

[29] B. D. Cullity, S.R. Stock, Elements of X-ray Diffraction, Prentice Hall, (2001) pp- 170.

[30] H. Hovel, S. Fritz, A. Hilgar, U. Kreibig, M. Vollmer, Phys. Rev. B. **48**, 18178 (1993).

[31] S. Link, M. A. El-Sayed, J. Phys. Chem. B **103**, 8410 (1999).

[32] U. Kreibig, L. Genzel, Surface Sci. **156**, 678 (1985).

[33] P. Mulvaney, Langmuir **12**, 788 (1996).

[34] A. C. Templeton, J. J. Pietron, R.W. Murray, P. Mulvaney, J. Phys. Chem. B **104**, 564 (2002).

[35] G. S. Agarwal, S. S Jha, Solid State Comm. **41**, 499 (1982).

[36] I.V.Kityk, A.Umar, M.Oyama. Physica E: Low-dimensional Systems and Nanostructures. **28**, 178 (2005).

[37] M. H. Rouillat, I.R. Antoine, E. Benichou, P. F. Brevet, Analy. Sci. **17**, 235 (2001).

[38] S.Shin, M Ishigame, J.Chem. Phys. **89**, 1892 (1998).

[39] S. Kielich, Lalanne, J.R. Martin, Phys. Rev. Lett. **26**, 1295 (1971).

[40] M.C. Flipse, de jonge R, R.H. Woudenberg, A.W. Marsman, C.A van Walree, L.W. Jenneskens, Chem. Phys. Lett. **245**, 297 (1995).

[41] J.P. Neddersen, S.A. Mounter, J.M.Bostick, C.K. Johnson, J. Chem. Phys. **90**, 4719 (1989).

[42] Yu Zhang, Xin Wang, Degang Fuuhong Lu, Journal of Physics and Chemistry of Solids **62**, 903 (2001).

[43] K.Clay, E.Hendrickx, M. Trient, A.Persoons, J. Mol. Liq. **67**, 133 (1995).

[44] M. Jacobsohn, U.Banin, J.Phys. Chem. 104, (2000)1.

*Corresponding author: jwd.physics@coep.ac.in